Application of novel metal–organic frameworks containing sulfonic acid pendings in synthesis of chromeno[4,3-d]pyrimidines *via* back to back anomeric based oxidation

Fatemeh Jalili [a], Hassan Sepehrmansourie [a], Mahmoud Zarei [b], Mohammad Ali Zolfigol [a], Ardeshir Khazaei [a], Mohammad Ali As'Habi [c]

[a] Department of Organic Chemistry, Faculty of Chemistry, Bu-Ali-Sina University, 6517838965 Hamedan, Iran
[b] Department of Chemistry, Faculty of Science, University of Qom, Qom 37185-359, Iran
[c] Department of Phytochemistry, Medicinal Plant and Drugs Research Institute, Shahid Beheshti University, Evin, Tehran 1983963113, Iran

ABSTRACT

Through task-specific design and synthesis of mesoporous catalysts, we introduce a novel metal–organic framework serving as a heterogeneous catalyst. In this study, Co(BDC-NH(CH$_2$)$_3$SO$_3$H) was meticulously prepared through the condensation reaction of 1,4-butane sultone and Co(BDC-NH$_2$) utilizing a post-modification method. The thorough examination of these parameters ensures a detailed understanding of the catalyst's properties. Subsequently, the catalytic activity was explored in the synthesis of chromeno[4,3-*d*]pyrimidine derivatives employing a cooperative vinylogous anomeric-based oxidation mechanism. This research not only presents a new and efficient catalyst but also contributes valuable insights into the synthesis of biologically relevant chromeno [4,3-*d*]pyrimidine derivatives.

1. Introduction

Metal-organic frameworks (MOFs) have emerged as a highly promising and innovative framework in the past century, owing to their nanoscale channels and pore structures akin to zeolites (Dhakshinamoorthy et al., 2020, Zhang et al., 2021). These materials consist of metal or metallic clusters coordinated with polyhedral organic ligands, offering a unique structural foundation (Safaei et al., 2019). The augmentation of surface area, pore volume, and architectural flexibility in metal–organic frameworks has opened up new avenues in research, particularly in the development of novel materials for applications in catalytic processes, gas separation, adsorption, and drug delivery (MacGillivray, 2010, Biswas et al., 2012, Furukawa et al., 2013, Yang et al., 2015, Sepehrmansourie, 2021, Ahmadi et al., 2022, Sepehrmansourie et al., 2023). In pursuit of these applications, the post-modification method has emerged as a groundbreaking approach for the preparation of heterogeneous catalysts. Consequently, this methodology forms the basis for a comprehensive discussion on the potential advantages of metal–organic frameworks (MOFs) as heterogeneous catalysts (Dhakshinamoorthy and Garcia, 2014, Xu et al., 2019, Bassanini et al., 2020, Dhakshinamoorthy et al., 2020, Zhang et al., 2020, Arabbaghi et al., 2021, Gao et al., 2022, Sepehrmansourie et al., 2022, Tavakoli et al., 2022).Among metal-based frameworks, those based on cobalt (Co), particularly MOFs, have garnered increased research attention in the past decade, with a focus on oxidation and the synthesis of organic compounds (Masoomi et al., 2015, Yang and Gates, 2019, Sepehrmansourie et al., 2021, Zhang et al., 2021). Notably, the post-modification of cobalt-based metal–organic frameworks is highly esteemed, as catalysts synthesized through this strategy demonstrate enhanced catalytic efficiency (Yu et al., 2014, Sepehrmansourie et al., 2021). The synthesis of *N*-heterocyclic compounds via the Hantzsch method encompasses a diverse array of materials exhibiting significant biological activity. These compounds find application in the treatment of various severe ailments, including antimicrobial interventions (Furdui et al., 2014), cancer therapeutics (Boselli et al., 2014), malaria treatment (Bueno et al., 2016), anticonvulsant drugs (Kumar et al., 2010), antifungal agents (Zhang et al., 2014), HIV medications (Metobo et al., 2006), anti-tumor drugs (Ahmed et al., 2009), antioxidants (Al-Omar et al., 2005), antihypertensive medications (Lang and Wenk, 1988), and urinary incontinence treatments (Catlin et al., 2004). Concurrently, chromeno[4,3-d]pyrimidine derivatives represent highly versatile chromene structures with widespread applications, serving as
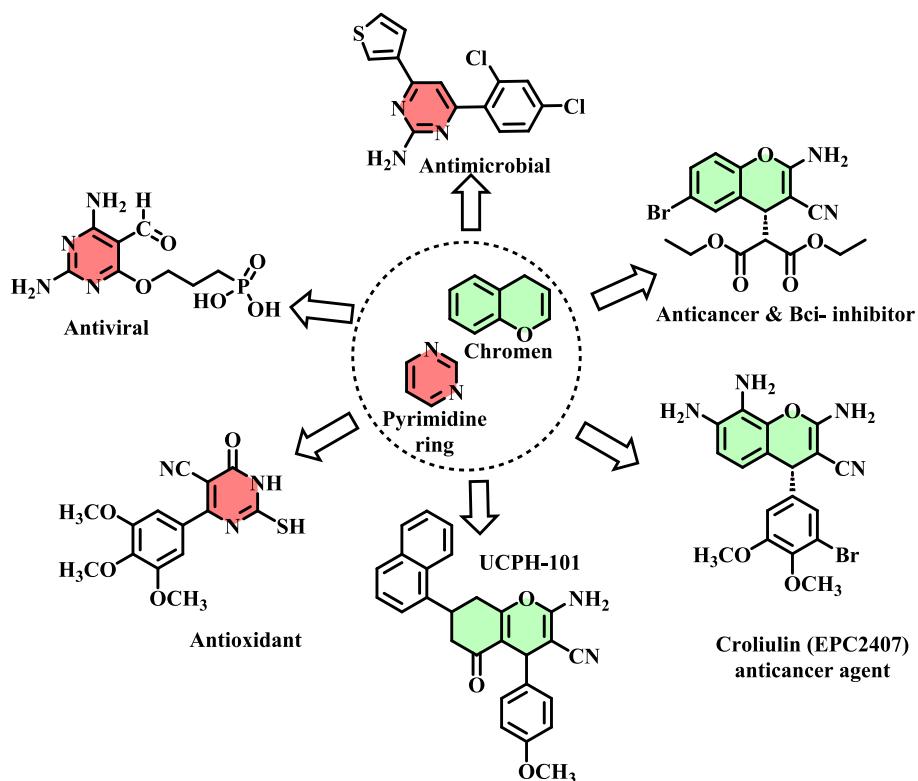
Scheme 1. Structures of compounds with pyridine and chromene have been used as a drug candidate.

anti-cancer agents, anti-tumor compounds, anti-AIDS medications, and possessing various other biological properties (Kamdar et al., 2011, Rajanarendar et al., 2012, Abd El-Mawgoud et al., 2018). Additionally, heterocyclic structures incorporating pyrimidine and chromene have been identified as promising drug candidates (Scheme 1). Consequently, researchers are motivated to explore and synthesize diverse compounds containing chromene and pyrimidine rings for their potential pharmacological activities(Aly and Kamal, 2012, Hese et al., 2017, Yavuz et al., 2021).

Stereoelectronic effects play a pivotal role in advancing synthesis methods and unraveling mechanisms in organic chemistry. This phenomenon involves a convergence of interactions encompassing orbitals, electrostatics, and steric factors in acetals (Miljkovic, 2009, Miljkovic and Miljković 2009, Hese et al., 2017, Yarie, 2020). Within a plethora of heterocyclic structures containing nitrogen and oxygen atoms, the hyperconjugative interaction between anti-bonding orbitals and lone pairs is known as the anomeric effect. The reported theory for the development of the anomeric effect (AE) concept had been proposed that sharing the lone pair's electrons of heteroatoms (X: N, O) to the anti-bonding orbital C-Y ($n_X \rightarrow \sigma^*_{C-Y}$) and weakened it. Similarly,

interactions involving double bonds and anti-bonding orbitals are termed vinylogous anomeric effects (**Figure S1**) (Atkins, 1980, Erhardt et al., 1980, Erhardt and Wuest, 1980) Conversely, the Cannizzaro reaction and the oxidation/reduction of NADP+/NADPH or NAD+/NADH systems introduce a novel mechanism by sharing electrons into the anti-bonding orbital, weakening it, and giving rise to what is termed anomeric-based oxidation (ABO). (Tabacchi et al., 2007, Hamasaka et al., 2015, He et al., 2016, Bai et al., 2017, Zhao et al., 2017). In this context, there is a significant demand for the synthesis of biological compounds through the cooperative vinylogous anomeric-based oxidation concept (**Figure S2**) (Afsar et al., 2018, Babaee et al., 2018, Zolfigol et al., 2018, Kalhor et al., 2019, Afsar et al., 2020, Babaee et al., 202, Kalhor et al., 2021, Naseri et al., 2021, Sepehrmansourie et al., 2021). This concept has yielded remarkable results and gained approval from various research groups (Zefirov and Shekhtman, 1971, Dondoni and Marra, 2000, Alabugin et al., 2021, Zippel et al., 2021). Recently, a comprehensive review of the role of these concepts in organic reactions has been conducted (Alabugin et al., 2021). In multi-component reactions, several raw materials are combined and react simultaneously with each other, facilitating the creation of new compounds through a
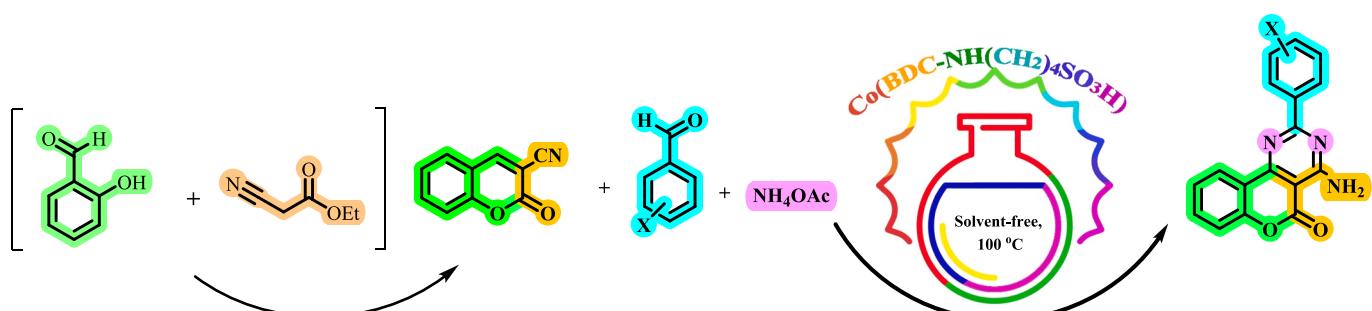
Scheme 2. Preparation of chromeno[4,3-*d*]pyrimidine derivatives using Co(BDC-NH(CH$_2$)$_4$SO$_3$H) as a catalyst.
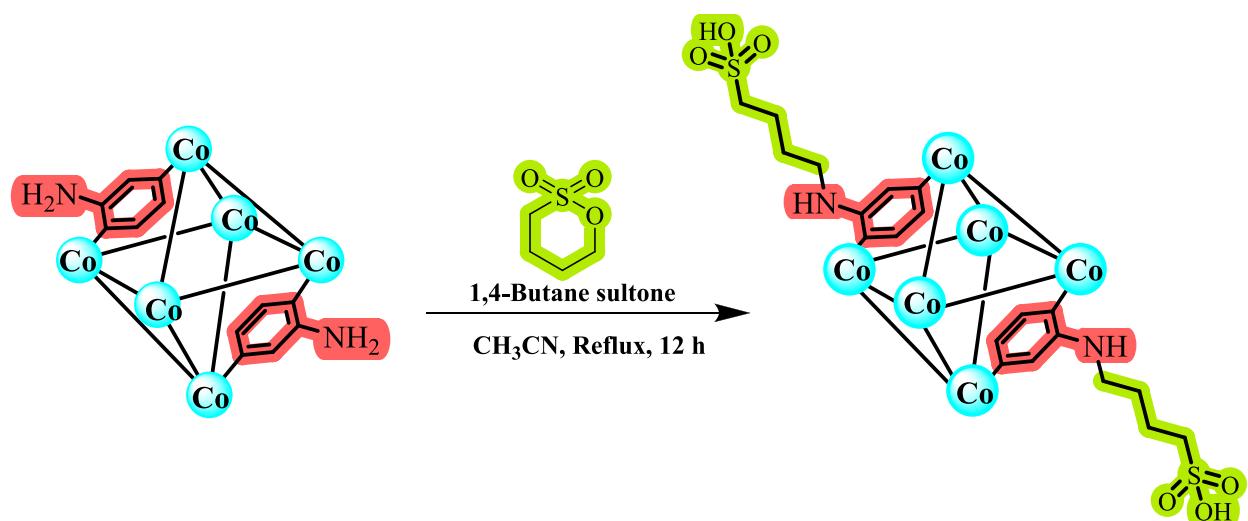
Scheme 3. Preparation of Co(BDC-NH(CH$_2$)$_4$SO$_3$H).

straightforward approach. Despite its introduction several decades ago, this method endures due to its efficiency and ease of application. The utilization of various catalysts has further enhanced the potential for synthesizing elaborate compounds in multicomponent reactions. (Saghanezhad et al., 2017, Sayahi et al., 2018, Sayahi et al., 2018, Sayahi et al., 2019, Sayahi et al., 2019, Sayahi et al., 2020, Moavi et al., 2021, Sayahi et al., 2021, Sayahi et al., 2021, Sayahi et al., 2021, Sayahi et al., 2022, Sayahi et al., 2022, Buazar et al., 2023, Sayahi et al., 2023).

In a recent development of heterogeneous catalysts Co(BDC-NH(CH$_2$)$_4$SO$_3$H) have been specifically engineered and produced based on their distinctive characteristics, including porosity, thermal stability, high surface area, and presence of sulfonic acid groups. These catalysts exhibit remarkable catalytic potential in the synthesis of chromeno[4,3-*d*]pyrimidine derivatives. chromeno[4,3-*d*]pyrimidine compounds have

garnered significant attention in scientific research due to their noteworthy biological properties. In light of this, we have achieved successful synthesis of chromium compounds with remarkable efficiency, minimal time requirement, and convenient separation. This accomplishment has been made possible by utilizing the catalyst Co(BDC-NH(CH$_2$)$_4$SO$_3$H) developed in a condensation reaction involving ethyl cyanoacetate, salicyl aldehyde, ammonium acetate, and various aldehydes (Scheme 2). Furthermore, through an in-depth investigation of the reaction mechanism, we have expanded our understanding of the anomeric-based oxidation mechanism in the course of synthesis of chromium compounds.
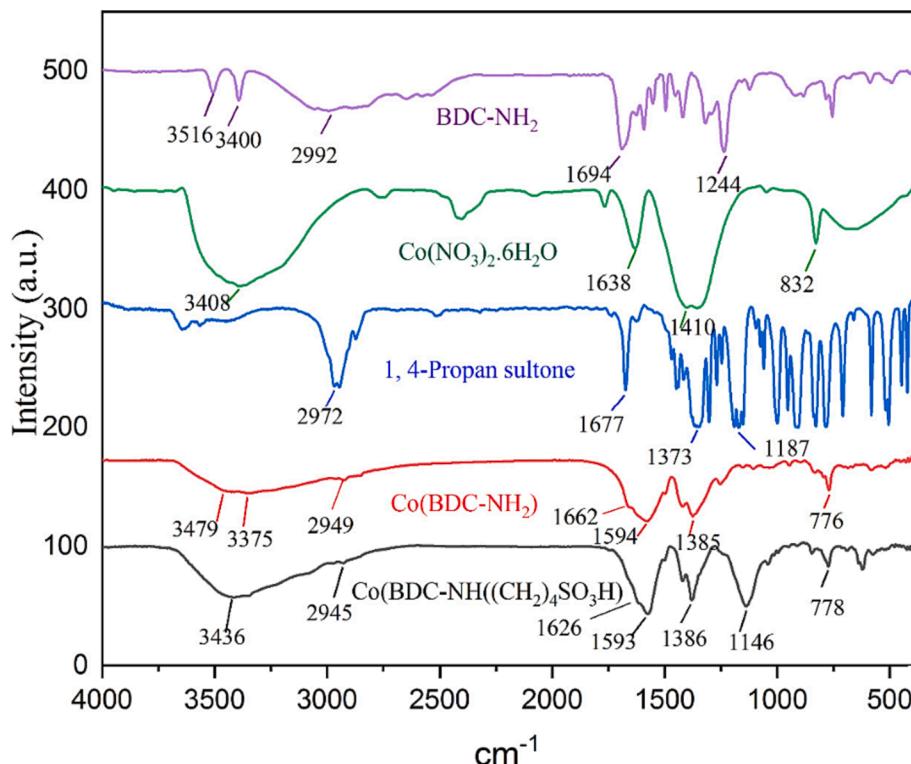

Fig. 1. Comparison FT-IR spectra of starting materials and Co(BDC-NH(CH$_2$)$_4$SO$_3$H).
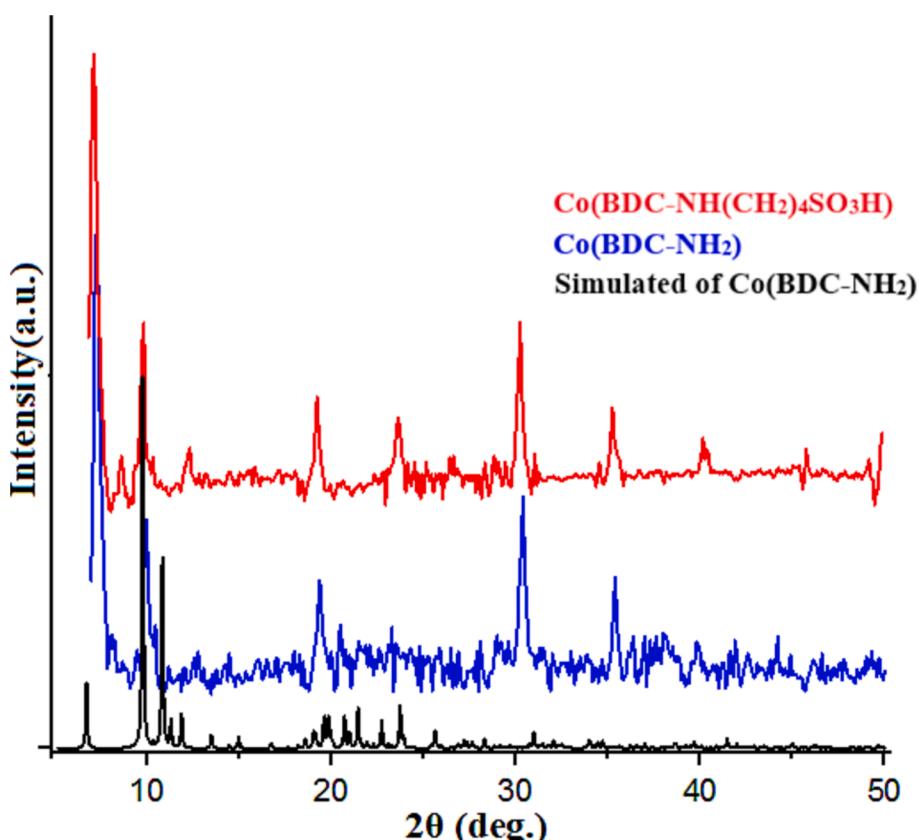
Fig. 2. Comparison XRD pattern of Co(BDC-NH$_2$), Co(BDC-NH(CH$_2$)$_4$SO$_3$H) and simulated of Co(BDC-NH$_2$).

2. Results and discussion

In our exploration of the catalytic potential of modified metal–organic frameworks (MOFs) using a post-modification approach (Babaee et al., 2020, Sepehrmansouri et al., 2020, Babaee et al., 2021, Kalhor et al., 2021, Naseri et al., 2021, Jalili et al., 2022), we introduce a novel approach for the design and synthesis of Co(BDC-NH(CH$_2$)$_4$SO$_3$H) utilizing metal–organic frameworks incorporating sulfuric acid groups. The desired catalyst, Co(BDC-NH(CH$_2$)$_4$SO$_3$H), was synthesized by reacting Co(BDC-NH$_2$) with 1,4-butanesultone in acetonitrile. (Scheme 3). A comprehensive analysis of the porous catalyst's structure and morphology was conducted, confirming its characteristics through various techniques such as Fourier transform infrared spectroscopy (FT-IR), elemental mapping analysis (EDX), scanning electron microscopy (SEM), X-ray spectroscopy (XRD), thermal gravimetric analysis (TG), derivative thermal gravimetric analysis (DTG), N_2 adsorption–desorption isotherm (BET), Transmission electron microscopes (TEM) and BJH. Subsequently, Co(BDC-NH(CH$_2$)$_4$SO$_3$H) was explored as a catalyst in the synthesis of chromeno[4,3-*d*]pyrimidine derivatives employing the cooperative vinylogous anomeric-based oxidation concept.

| Element	Weight%	Atomic%
C K	32.92	45.87
N K	5.26	6.28
O K	36.56	38.25
S K	10.19	5.32
Co K	15.07	4.28
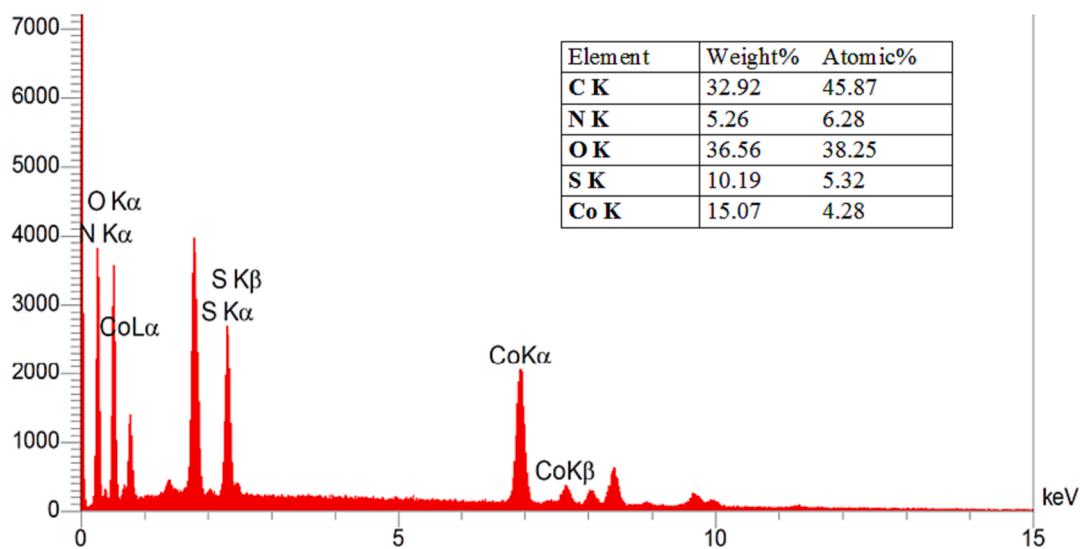
Fig. 3. Energy dispersive X-ray (EDX) of Co(BDC-NH(CH$_2$)$_4$SO$_3$H).
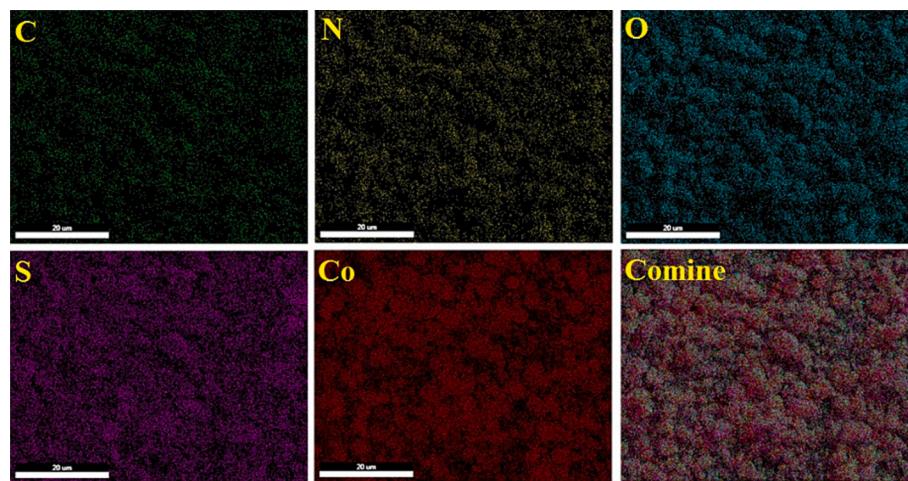
Fig. 4. Elemental mapping analysis of Co(BDC-NH(CH$_2$)$_4$SO$_3$H) as a catalyst.
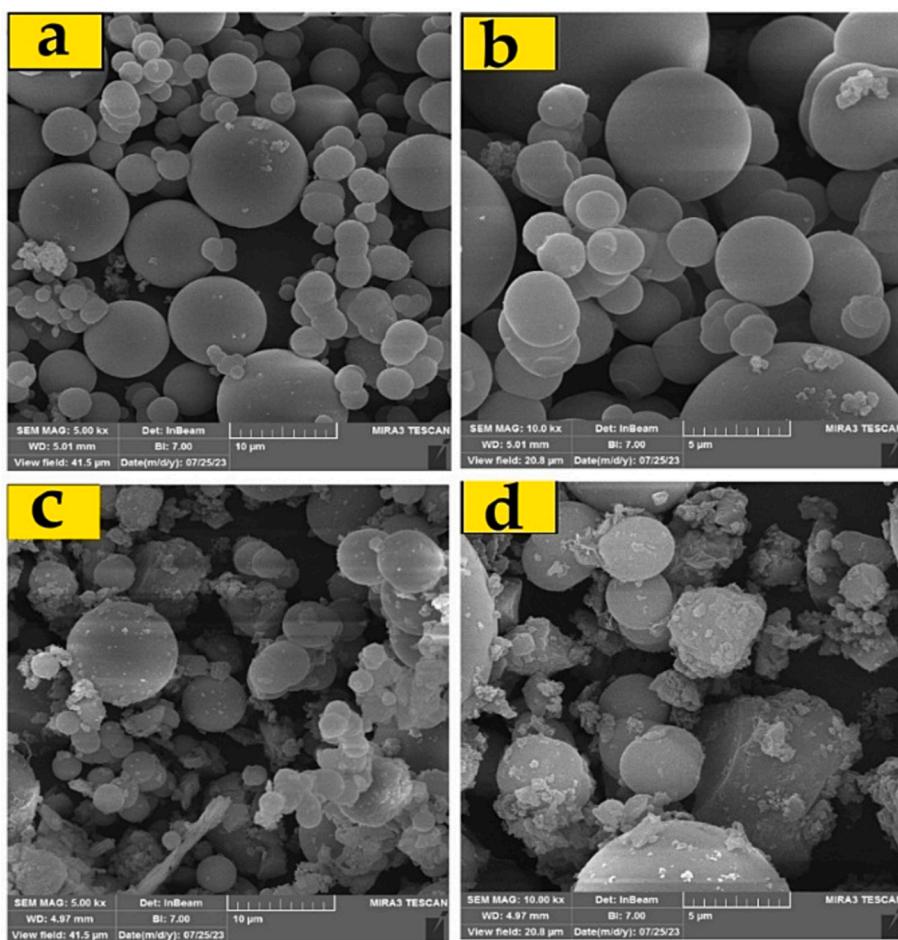
Fig. 5. Scanning electron microscopy (SEM) of Co(BDC-NH$_2$) (a & b) and Co(BDC-NH(CH$_2$)$_4$SO$_3$H) (c & d).

2.1. Investigating the structure and morphology of the catalyst

In Fig. 1, the FT-IR spectra of Co(NO$_3$)$_2$·6H$_2$O, 2-aminoterephthalic acid (BDC-NH$_2$), 1,4-butanesultone, Co(BDC-NH$_2$), and Co(BDC-NH(CH$_2$)$_4$SO$_3$H) were meticulously compared. Notably, the broad peak in the range of 2600–3500 cm^{-1} is attributed to the presence of OH in the SO$_3$H groups. Furthermore, the absorption peak at 1146 cm^{-1} corresponds to the stretch bands of O-S. Aromatic C–H and C = C stretches bands are observed at 2945 and 1588 cm^{-1}, respectively. Additionally, the peaks associated with Co-O in octahedral CoO$_6$ are evident at 776 cm^{-1}. Subsequently, absorption bands at 3400 and 3516 cm^{-1} are linked to the NH$_2$ group of (BDC-NH$_2$). Through analysis of the alterations observed in the Fourier-transform infrared (FT-IR) spectrum of the unprocessed substances and at every stage of the catalyst synthesis, one may deduce that the functional entity of the metal–organic framework substrate has undergone modification, resulting in the acquisition
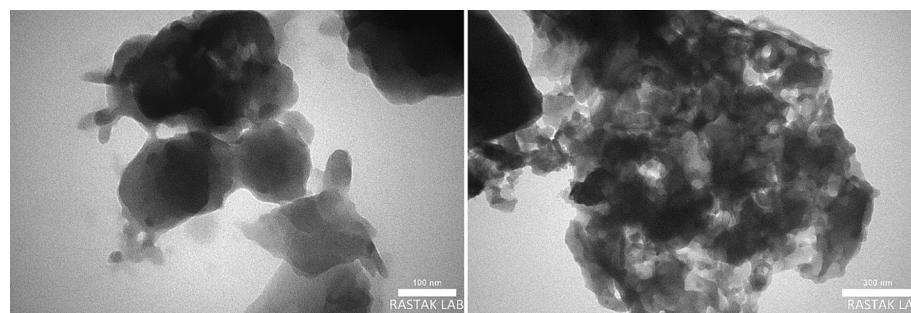
Fig. 6. Transmission electron microscopes (TEM) of Co(BDC-NH(CH₂)₄SO₃H).
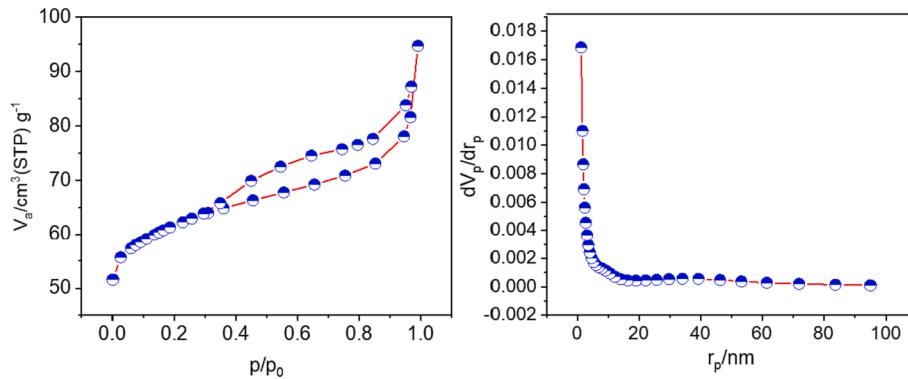
Fig. 7. N_2-adsorption/desorption isotherm (BET) and the pore size distribution plot based on BJH method for Co(BDC-NH(CH₂)₄SO₃H).

of the proposed configuration for the catalyst.

The structural integrity of Co(BDC-NH(CH₂)₄SO₃H) underwent verification through XRD analysis (Fig. 2). The comparison of the X-ray diffraction (XRD) patterns demonstrates congruity with previously documented observed data and verifies the arrangement of Co(BDC-NH(CH₂)₄SO₃H), as depicted in the study by Yang et al., 2015. The growth pattern of crystal plates shows that the metal–organic framework is well prepared and its crystal plates were not destroyed during the post-

modification stage of this structure to make it functional.

In an additional examination, the elemental composition of Co(BDC-NH(CH₂)₄SO₃H) was analyzed using the energy dispersive X-ray spectroscopy (EDX) technique, revealing the presence of cobalt, carbon, nitrogen, sulfur, and oxygen atoms (Fig. 3). Also, the presence of these elements and their uniform distribution on the surface of the catalyst was well confirmed by the elemental mapping analysis (Fig. 4). The morphology of both Co(BDC-NH₂) and Co(BDC-NH(CH₂)₄SO₃H) was
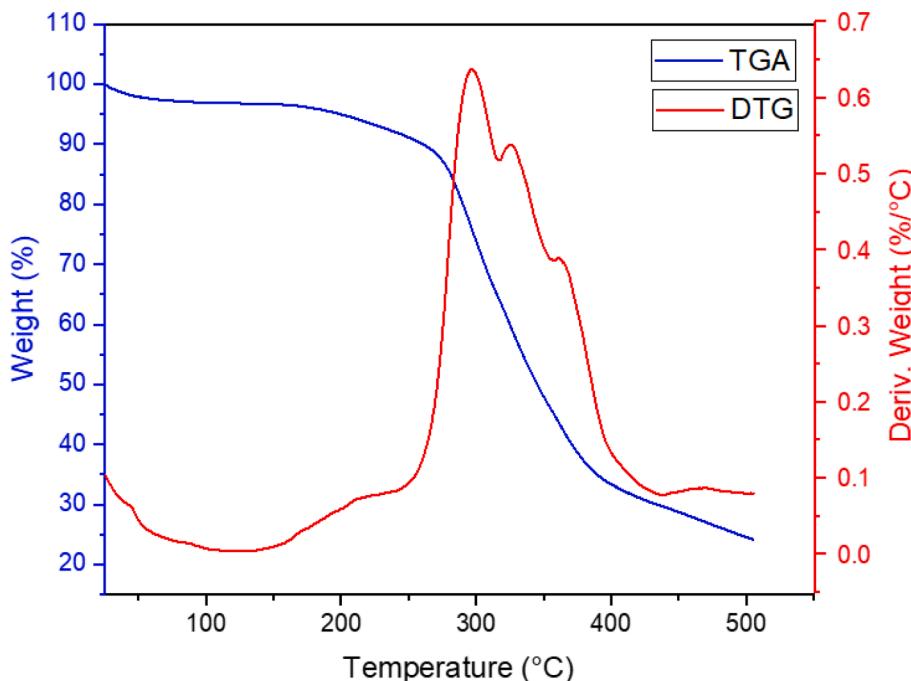
Fig. 8. Thermal gravimetric analyses (TGA) and derivative thermal gravimetric (DTG) analyses of Co(BDC-NH(CH₂)₄SO₃H).

Table 1
The effect of different amounts of catalysts, temperature and solvent (5 mL) in the synthesis of chromeno[4,3-*d*]pyrimidine.
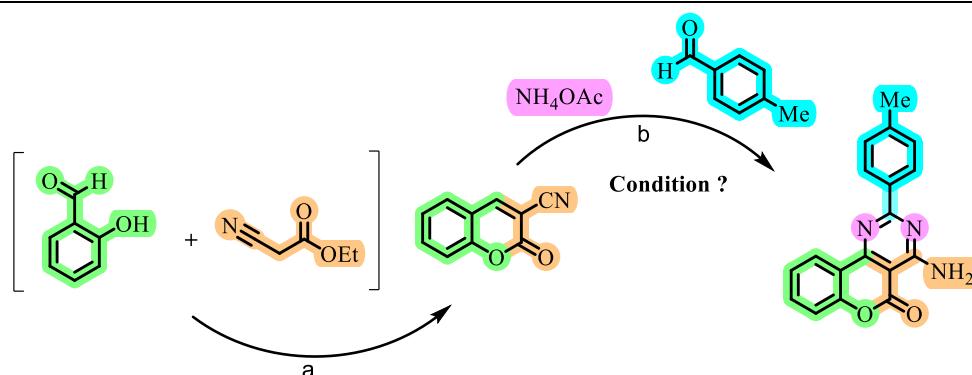
| Entry	Catalyst (mg)	Amine source	Temperature (°C)	Solvent	Time (min.)	Yield (%)	TOF	TON
1	–	NH$_4$OAc	100	Solvent-free	60	Trace	–	–
2	5	NH$_4$OAc	100	Solvent-free	60	45	0.15	4.5
3	**10**	**NH$_4$OAc**	**100**	**Solvent-free**	**35**	**88**	**0.25**	**8.8**
4	15	NH$_4$OAc	100	Solvent-free	35	88	0.17	58
5	10	NH$_4$OAc	25	Solvent-free	60	Trace	–	–
6	10	NH$_4$OAc	50	Solvent-free	60	52	0.08	5.2
7	10	NH$_4$OAc	70	Solvent-free	60	67	0.11	6.7
8	10	NH$_4$OAc	Reflux	DMF	50	70	0.14	7.0
9	10	NH$_4$OAc	Reflux	CH$_3$CN	120	62	0.05	6.2
10	10	NH$_4$OAc	Reflux	H$_2$O	50	55	0.11	5.5
11	10	NH$_4$OAc	Reflux	EtOH	35	48	0.14	4.8
12	10	NH$_4$OAc	Reflux	CH$_2$Cl$_2$	120	–	–	–
13	10	NH$_4$OAc	Reflux	EtOAc	60	58	0.1	5.8
14	10	(NH$_4$)$_2$SO$_4$	100	Solvent-free	60	Trace	–	–
15	10	NH$_4$Cl	100	Solvent-free	60	–	–	–
16	10	NH$_4$F	100	Solvent-free	60	–	–	–
17	10	(NH$_4$)$_2$CO$_3$	100	Solvent-free	60	50	0.08	5.0
18	10	NH$_4$HCO$_2$	100	Solvent-free	60	45	0.07	4.5
19	10^c	NH$_4$OAc	100	Solvent-free	60	40	0.07	4.0
20	10^d	NH$_4$OAc	100	Solvent-free	60	Trace	0	0
21	10^e	NH$_4$OAc	100	Solvent-free	40	50	0.12	5.0

[a]Reaction conditions: Salicylaldehyde (1.0 mmol, 0.122 g), Ethyl cyanoacetate (1.0 mmol, 0.113 g) and NH$_4$OAc or Co(BDC-NH(CH$_2$)$_4$SO$_3$H) as a catalyst, solvent-free at 100 °C; [b] Reaction conditions: 4-Methylbenzaldehyde (1.0 mmol, 0.12 g), NH$_4$OAc (3.0 mmol, 0.234 g) and 2-oxo-2*H*-chromene-3-carbonitrile (1.0 mmol, 0171 g), C: BDC-NH$_2$, d: Co(NO$_3$)$_3$·6H$_2$O, e: Co(BDC-NH$_2$).

scrutinized through scanning electron microscopy (SEM) (Fig. 5). As depicted in Fig. 5, the particle morphology of the desired Co(BDC-NH(CH$_2$)$_4$SO$_3$H) remains spherical, demonstrating stability and maintaining its structure after functionalization. Morphology of catalyst Co(BDC-NH(CH$_2$)$_4$SO$_3$H) was investigated with transmission electron microscope (TEM) (Fig. 6). The TEM images obtained from the catalyst Co(BDC-NH(CH$_2$)$_4$SO$_3$H) show that the morphology is spherical, which confirms the images obtained from the SEM. The existence of such a morphology creates a suitable substrate for catalytic activity because in this case the raw materials of the reaction are well placed on this substrate and the catalyst plays its role better.

The porosity and surface area of Co(BDC-NH(CH$_2$)$_4$SO$_3$H) were examined through N$_2$ adsorption–desorption analysis (Fig. 7). The BET data yielded a surface area of 235 m^{2}g^{-1}, while the total pore volume was determined to be 0.15 cm^{3}g^{-1}, indicating the porous nature of Co(BDC-NH(CH$_2$)$_4$SO$_3$H). Utilizing the Barrett-Joyner-Halenda (BJH) method, the pore size distribution was obtained, revealing predominant pore sizes between 1 and 10 nm, with an average pore size of 2.5 nm. This analysis affirms the mesoporous structure of Co(BDC-NH(CH$_2$)$_4$SO$_3$H), consistent with the observed hysteresis loop. The existence of a porous structure as well as a suitable surface area created for the catalyst has been an important factor in advancing the catalytic goals of the target catalyst.

To assess the thermal stability of Co(BDC-NH(CH$_2$)$_4$SO$_3$H), thermal gravimetric (TGA) and derivative thermal gravimetric (DTG) analyses were conducted (Fig. 8). The TGA pattern displayed three distinct

decline stages for Co(BDC-NH(CH$_2$)$_4$SO$_3$H). The initial weight loss of 5–6 % was attributed to the removal of moisture and organic solvents used during the synthesis. The primary stage of weight loss, occurring at temperatures between 270 and 320 °C, corresponds to the release of SO$_2$ (Bhardwaj et al., 2016, Saikia and Saikia, 2016). Notably, the TGA results indicate that as the temperature increases to 400 °C, the structure and morphology of the metal–organic framework undergo complete degradation. This analysis underscores that the operational temperature of Co(BDC-NH(CH$_2$)$_4$SO$_3$H) is limited to temperatures below 250 °C.

2.2. Optimum conditions of the synthesis chromeno[4,3-d]pyrimidine derivatives

Once the structure and topography of Co(BDC-NH(CH$_2$)$_4$SO$_3$H) were confirmed, it was employed as a heterogeneous catalyst for the synthesis of chromeno[4,3-*d*]pyrimidine derivatives featuring pyrimidine and chromene structures. The synthesis involved the reaction of 2-oxo-2*H*-chromene-3-carbonitrile (1 mmol, 0.171 g), *p*-methyl benzaldehyde (1 mmol, 0.12 g), and ammonium acetate (3 mmol, 0.234 g) as a model reaction for optimization purposes. Table 1 summarizes the results, revealing that the optimal conditions for the preparation of chromeno[4,3-*d*]pyrimidine derivatives were achieved in the presence of 10 mg Co(BDC-NH(CH$_2$)$_4$SO$_3$H) as a catalyst under solvent-free conditions (Table 1, entry 3). The exploration extended to using various solvents such as DMF, CH$_3$CN, H$_2$O, EtOH, CH$_2$Cl$_2$, and EtOAc (5 mL) in the presence of 10 mg of catalyst, but no improvement was observed

1a
Mp °C: 265–268 (266–268)
(Sakurai et al., 1971)
Yield: 85 %, Time: 40 min.

2a
Mp °C: 254–256 (254–257)
(Sakurai et al., 1971)
Yield: 90 %, Time: 30 min.

3a
Mp °C: 278–280(277–280)
(Sakurai et al., 1971)
Yield: 88 %, Time:35 min.

4a
Mp °C: 260–261 (262–264)
(Sakurai et al., 1971)
Yield:91 %, Time: 35 min.

5a
Mp °C: 230–231 (229–231)
(Sakurai et al., 1971)
Yield: 81 %, Time:45 min.

6a
Mp °C: 254–256 (254–256)
(Sakurai et al., 1971)
Yield: 71 %, Time:60 min.

7a
Mp °C: 230–232 (225–228)
(Sakurai et al., 1971)
Yield: 83 %, Time: 65 min.

8a
Mp °C: 250–251
Yield: 84 %, Time: 50 min.

9a
Mp °C: >300
Yield: 82 %, Time: 60 min.

10a
Mp °C: >300
Yield: 86 %, Time: 45 min.

11a
Mp °C: >300
Yield: 92%, Time: 30 min.

12a
Mp °C: >300
Yield: 88%, Time: 30 min.

13a
Mp °C: 281–283
Yield: 87 %, Time: 55 min.

14a
Mp °C: 290–293
Yield: 80 %, Time:65 min.

15a
Mp °C: >300
Yield: 85 %, Time: 40 min.

16a
Mp °C: >300
Yield: 84 %, Time: 45 min.

17a
Mp °C: 295–297
Yield: 82 %, Time: 40 min.

18a
Mp °C: 290–292
Yield: 90 %, Time: 30 min.

19a
Mp °C: 288–290
Yield: 85 %, Time: 45 min.

Fig. 9. The synthesis of chromeno[4,3-*d*]pyrimidine using Co(BDC-NH(CH$_2$)$_4$SO$_3$H) as a catalyst.

Table 2
The evaluation of various catalysts for the synthesis of chromeno[4,3-*d*]pyrimidine in comparison with Co(BDC-NH(CH$_2$)$_4$SO$_3$H) under solvent-free condition.

Entry	Catalyst	Amount of catalyst (mg)	Time (min)	Yield (%)[a]	TOF	TON
1	*p*-TSA	10 mol%	45	66	0.15	6.6
2	Al(HSO$_4$)$_3$	10 mol%	45	75	0.17	7.5
3	H$_3$[p(W$_3$O$_{10}$)$_4$].XH$_2$O	10 mol%	60	25	0.04	2.5
4	Fe$_3$O$_4$	10	55	30	0.05	3.0
5	MIL-101(Cr)-N(CH$_2$PO$_3$H$_2$)$_2$ (Babaee et al., 2020)	10	45	73	0.16	7.3
6	[Zr-UiO-66-PDC-SO$_3$H]Cl (Naseri et al., 2021)	10	35	78	0.22	7.8
7	[Zr-UiO-66-PDC-SO$_3$H]FeCl$_4$ (Jalili et al., 2022)	10	50	74	0.15	7.4
8	PCPs(Bi)N(CH$_2$PO$_3$H$_2$)$_2$ (Babaee et al., 2021)	10	45	72	0.16	7.2
9	[Py-SO$_3$H]Cl (Moosavi-Zare et al., 2013)	10	45	52	0.11	5.2
10	SSA (Zolfigol, 2001) (Sepehrmansourie, 2020)	10	45	50	0.11	5.0
11	[Phen(SO$_3$H)$_2$]Cl$_2$ (Babaee et al., 2018)	10 mol%	60	35	0.06	3.5
12	SBA-15/PrN(CH$_2$PO$_3$H$_2$)$_2$ (Jalili et al., 2020)	10	60	60	0.1	6.0
13	**Co(BDC-NH(CH$_2$)$_4$SO$_3$H)** **This work**	**10**	**35**	**88**	**0.25**	**8.8**

[a] : Isolated yield.

(Table 1, entries 8–13). Encouraged by these findings, a diverse range of pyrazolo [3,4-*b*] pyridine compounds were created under solvent-free conditions. Further investigations considered varying conditions, such as temperature changes and different catalyst amounts, as detailed in Table 1. After optimizing the reaction conditions for chromeno[4,3-*d*] pyrimidine synthesis, a variety of amine sources were explored to assess their impact on efficiency. According to the results in Table 1, the highest efficiency was achieved with ammonium acetate (Table 1, entry 3), while ammonium carbonate and ammonium format resulted in average efficiency (Table 1 entries 17–18). No product was observed with ammonium chloride and ammonium fluoride, and ammonium sulfate salt yielded negligible product (Table 1, entries 14–16). After identifying the optimal conditions through the model reaction chosen for chromeno[4,3-*d*]pyrimidine synthesis, BDC-NH$_2$, Co(NO$_3$)$_3$·6H$_2$O, and Co(BDC-NH$_2$) were employed as catalysts in the chromeno[4,3-*d*] pyrimidine synthesis (Table 1, entries 19–21). The outcomes indicate lower efficiency compared to the Co(BDC-NH(CH$_2$)$_4$SO$_3$H). Since the determination of TON and TOF is performed for homogeneous catalysts and is not easily definable for the heterogeneous catalysts in comparison to homogeneous ones or enzymes, this is due to the adsorption sites, which are commonly quantified through chemical adsorption of a suitable gas and the enumeration of surface metal atoms employed, do not necessarily align with the "active" sites. The reaction conditions on an atomic scale, as well as the precise configurations of atoms that constitute the active site, remain largely unknown for any heterogeneous reaction. It is highly plausible that distinct active sites may coexist, each operating at its own individual rate. Consequently, the determined TON and TOF values subsequently reflect an average measure of the overall catalytic activity (Vannice and Joyce, 2005).

To delve deeper into the synthesis of chromeno[4,3-*d*]pyrimidine derivatives, a comprehensive exploration involving a varied spectrum of aryl aldehydes, encompassing both electron-withdrawing and electron-releasing substituents, was undertaken. The results, as outlined in Fig. 9, underscored the effectiveness of Co(BDC-NH(CH$_2$)$_4$SO$_3$H) in facilitating the production of target molecules in high to excellent yields (71–92 %) within relatively short reaction times (30–65 min.). Several aliphatic aldehydes, including crotonaldehyde, heptanal, butyraldehyde, and acetaldehyde, were explored for the potential synthesis of chromium compounds. However, upon monitoring the reaction using TLC technique, no products were observed. The absence of product synthesis

with aliphatic aldehydes is attributed to their tendency to undergo condensation reactions.

To gauge the efficacy of the synthesized catalyst in the synthesis of chromeno[4,3-*d*]pyrimidine derivatives, reactions were conducted using 2-oxo-2*H*-chromene-3-carbonitrile (1 mmol, 0.171 g), *p*-methyl benzaldehyde (1 mmol, 0.12 g), and ammonium acetate (3 mmol, 0.234 g) with various inorganic and organic catalysts under optimal conditions (Table 2). The results presented in Table 2 unequivocally demonstrate that Co(BDC-NH(CH$_2$)$_4$SO$_3$H) outperforms other catalysts, emerging as the most effective catalyst for the synthesis of the desired product.

The superior efficiency of the designed catalyst, in contrast to both homogeneous and heterogeneous catalysts, can be attributed to the highest stability of the formed sulfonic acid functional group (carbon–sulfur bond). This stability surpasses that of other heterogeneous catalysts (entries 6, 7, 9, 11), characterized by weaker nitrogen-sulfur bonds. Additionally, the inclusion of sulfonic acid enhances the reaction rate more than catalysts containing phosphorous acid functional groups (entries 5, 8, 12).

2.3. Mechanism for the synthesis of chromeno[4,3-d]pyrimidine derivatives

The SO$_3$H functional group plays the role of acid catalyst in many organic reactions. Here, the goal was to design a porous solid catalyst with SO$_3$H acidic groups. These types of catalysts work well in activating different compounds by using their proper acidic property and are important in increasing the reaction rate. The proposed mechanism for the synthesis of chromeno[4,3-*d*]pyrimidine derivatives utilizing Co (BDC-NH(CH$_2$)$_4$SO$_3$H) as a catalyst is elucidated in Scheme 4. In the first step, the catalyst activate aldehyde, and NH$_3$ released from the ammonium acetate reacts with it to form the intermediate (I), accompanied by the elimination of a water molecule. Subsequently, intermediate (I) engages in a reaction with 2-oxo-2*H*-chromene-3-carbonitrile, serving as a Michael acceptor, to yield intermediate (II). The ensuing steps involve intramolecular cyclization and tautomerization of intermediate (II), leading to the formation of intermediate (III). In line with recent advancements, a novel concept involving negative hyperconjugation during the synthesis of molecules through susceptible intermediates, specifically termed anomeric-based oxidation, has been introduced (Zolfigol et al., 2015, Kiafar et al., 2016, Moosavi-Zare et al., 2016,
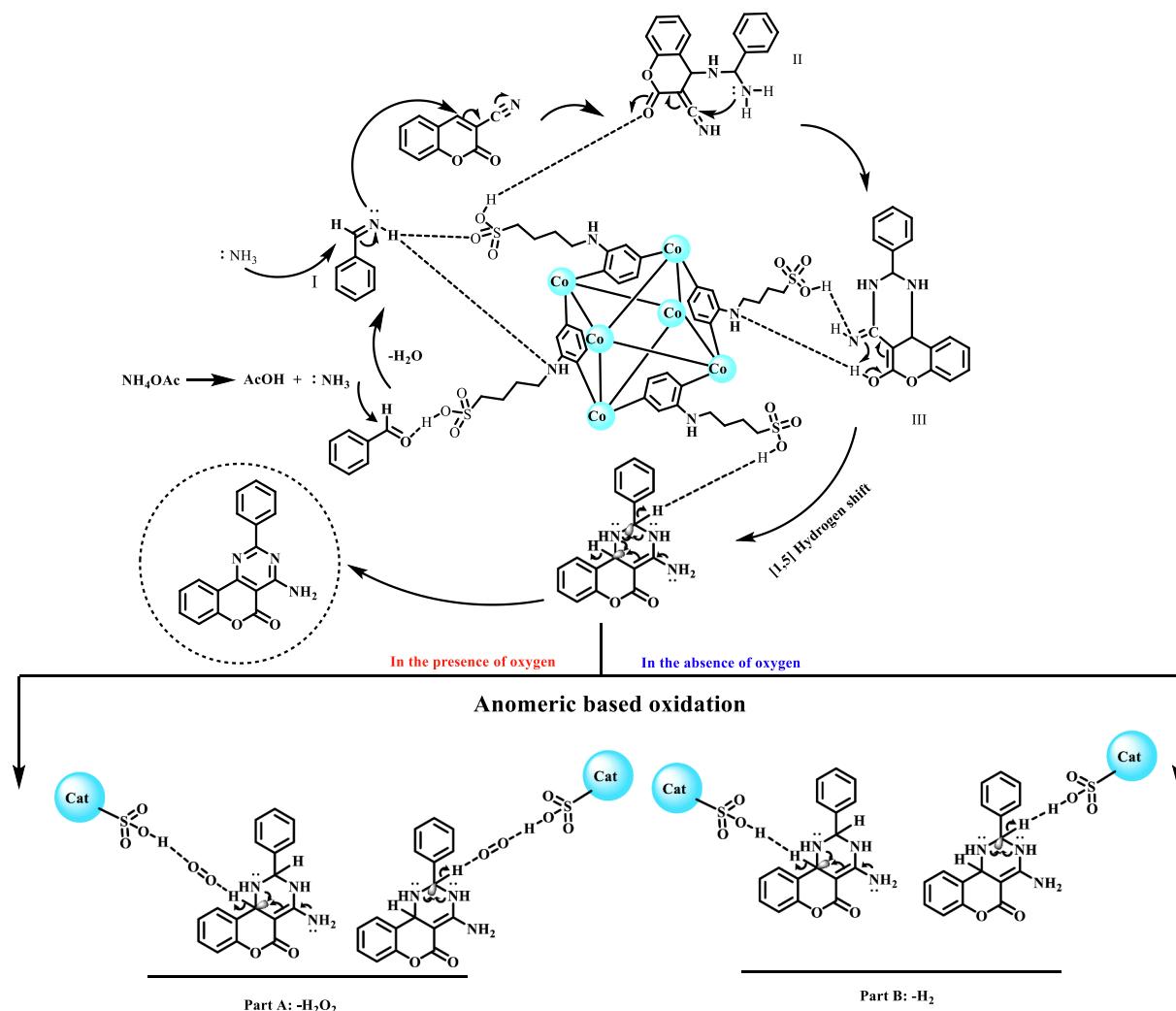
Scheme 4. Proposed mechanism for synthesis chromeno[4,3-*d*]pyrimidine using Co(BDC-NH(CH$_2$)$_4$SO$_3$H) as a catalyst.

Yarie, 2017, Zolfigol and Yarie, 2017, Zolfigol et al., 2018, Zolfigol et al., 2018, Jalili et al., 2020). These concepts have been comprehensively reviewed (Yarie, 2017, Yarie, 2020). According to the aforementioned concept, intermediate (III) undergoes hydride transfer and H$_2$ release through the interaction of lone pair electrons of N atoms and C = C bonds. Finally, intermediate (III) transforms into the desired product via a cooperative vinylogous anomeric-based oxidation, liberating a hydrogen molecule (–H$_2$) (Zolfigol and Yarie, 2017). The results obtained from the model reaction under argon, nitrogen, and oxygen atmospheres are consistent, validating the proposed mechanism.

2.4. Recyclability of Co(BDC-NH(CH$_2$)$_4$SO$_3$H)

The reusability of the described Co(BDC-NH(CH$_2$)$_4$SO$_3$H) for the preparation of chromeno[4,3-*d*]pyrimidine derivatives is depicted in Fig. 10. In this assessment, Co(BDC-NH(CH$_2$)$_4$SO$_3$H) was employed as a catalyst for the model reaction under the previously optimized conditions. The results presented in Fig. 10 demonstrate that Co(BDC-NH(CH$_2$)$_4$SO$_3$H) maintains its catalytic activity effectively for up to six runs, with no noticeable changes observed. The observed reduction in efficiency subsequent to catalyst reuse can be attributed to a decline in porosity levels, stemming from pore blockage. Additionally, the interaction between materials and intermediates with the functional groups of the catalyst leads to catalyst poisoning, which is the primary cause of decreased catalyst efficiency.

The structure and morphology of the reused catalyst were characterized using EDX and SEM techniques after six runs in the model reaction. The EDX analysis revealed that the presence of carbon, oxygen, nitrogen, sulfur, and cobalt elements in the structure of the recovered catalyst (Fig. 11). SEM images indicated that the morphology of the catalyst remained unchanged after six cycles of use and recovery, retaining its spherical structure (Fig. 12).

3. Experimental section

3.1. Materials and methods

The materials used, such as Cobalt(II) nitrate hexahydrate (Co(NO$_3$)$_2$·6H$_2$O) (Merck, 95 %), 2-aminoterephthalic acid (BDC-NH$_2$) (Sigma-Aldrich, 99 %), Butane sultone (Merck, 99 %), Ethyl cyanoacetate (Merck, 99 %), Salicylaldehyde (Merck, 99 %), Ethanol (C$_2$H$_5$OH) (Merck, 99 %), Dimethylformamide (DMF) (Merck, 99 %), Ammonium acetate (NH$_4$OAc) (Sigma-Aldrich, 99 %), Aldehyde derivatives (Merck, 99 % & Sigma-Aldrich, 99 %), and other materials (Merck), were reagent-grade and used without further purification.

Instrumental measurements included FT-IR analysis using a Perkin Elmer Spectrum Version 10.02.00 device for infrared spectra, melting points recorded on a Büchi B-545 apparatus in open capillary tubes, and NMR spectra (^{1}H NMR at 400 MHz, ^{13}C NMR at 100 MHz) recorded on a BRUKER Ultra shield FT-NMR spectrometer (δ in ppm). SEM analysis
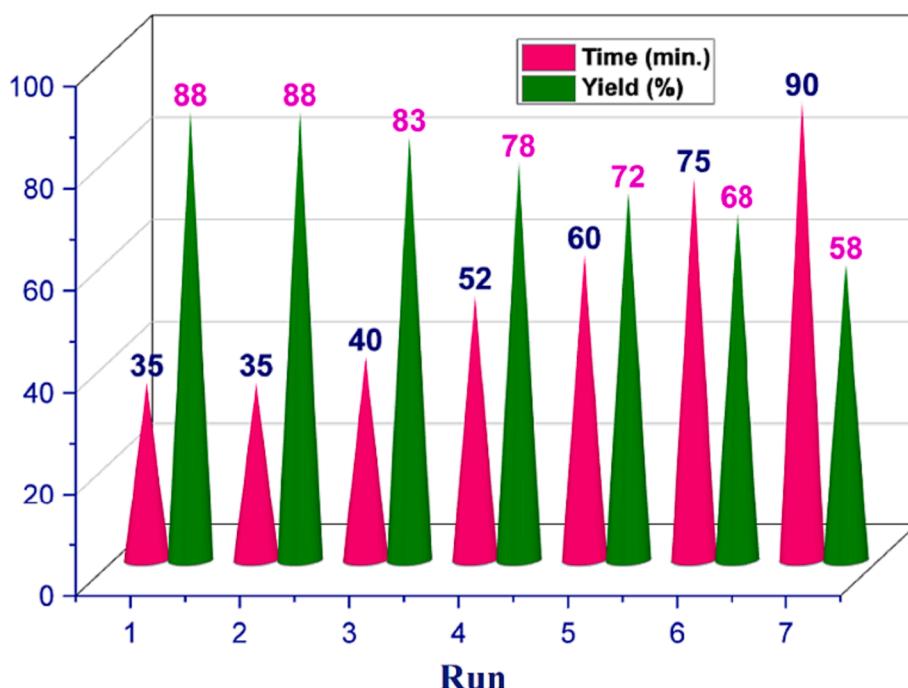
Fig. 10. Recyclability of Co(BDC-NH(CH$_2$)$_4$SO$_3$H) as a catalyst for the synthesis of chromeno[4,3-*d*]pyrimidines.

| Element	Weight%	Atomic%
C K	30.92	45.29
N K	6.20	6.88
O K	37.57	37.4
S K	11.15	6.07
Co K	14.16	4.36
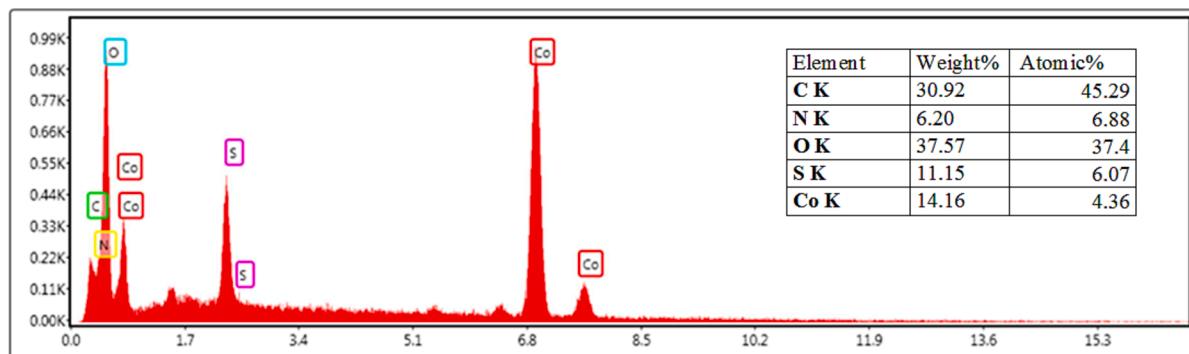
Fig. 11. Energy dispersive X-ray (EDX) of reused catalyst.

was conducted using a TESCAN scanning electron microscope (model: MIRA-II, Czechia). Thermal gravimetry (TGA) and differential thermal gravimetric (DTG) analyses were performed using a TA instrument (model: Q600). BET and BJH analyses were conducted by BEL (model: Belsorp Mini II). XRD analysis was carried out using a PHILIPS X-ray diffractometer (model: PW1730), and TEM analysis was performed using an EM 208S Transmission electron microscopy.

3.2. General procedure for the post-modification of Co(BDC-NH (CH$_2$)$_4$SO$_3$H)

Initially, Co(BDC-NH$_2$) was synthesized according to the previously reported method (Yang et al., 2015). For this purpose, a mixture of Co (NO$_3$)$_2$·6H$_2$O (2 mmol, 0.58 g), BDC-NH$_2$ (1 mmol, 0.18 g) and DMF (35 mL) and EtOH (10 mL) as solvent were stirred. After 5 min., the contents of both containers were placed in a 60 mL autoclave at 120 °C for 48 h. After cooling, the precipitate was washed several times with DMF and EtOH. Subsequently, in a 25 mL round-bottom flask, Co(BDC-NH$_2$) (0.2 g), 1,4-butane sultone (5 mmol, 0.68 g), and 10 mL of dry acetonitrile as the solvent were stirred for 12 h under reflux condition. When the reaction was complete, the mixture was cooled to 25 °C, and the resulting

purple solid was collected through centrifugation (3 × 1000 rpm). The purple sediment was washed with acetonitrile (3 × 5 mL) and then dried under vacuum at 80 °C to 0.23 g of Co(BDC-NH(CH$_2$)$_4$SO$_3$H) (Scheme 3). Inductively Coupled Plasma (ICP) analysis was used to measure the amount of cobalt metal present in the Co(BDC-NH(CH$_2$)$_4$SO$_3$H) structure, and the amount of cobalt 2.5 × 10^{-3} mol g^{-1} was obtained in the catalyst.

3.3. General procedure for the synthesis of chromeno[4,3-d]pyrimidine derivatives using Co(BDC-NH(CH$_2$)$_4$SO$_3$H) as a catalyst

For the synthesis of chromeno[4,3-*d*]pyrimidine derivatives using Co (BDC-NH(CH$_2$)$_4$SO$_3$H) as a catalyst, 2-oxo-2*H*-chromene-3-carbonitrile was initially prepared by the condensation reaction of salicylaldehyde (1 mmol, 0.122 g) and ethyl cyanoacetate (1 mmol, 0.113 g) following reported methodology (Scheme 5) (Sakurai et al., 1971). In a 10 mL round-bottomed flask, a mixture of 2-oxo-2*H*-chromene-3-carbonitrile (1 mmol, 0.171 g), benzaldehyde derivatives (1 mmol), ammonium acetate (3 mmol, 0.234 g), and Co(BDC-NH(CH$_2$)$_4$SO$_3$H) (10 mg) as a catalyst were stirred under solvent-free conditions at 100 °C. The reaction progress was monitored by TLC (*n*-hexane/ethyl acetate: 2/1).
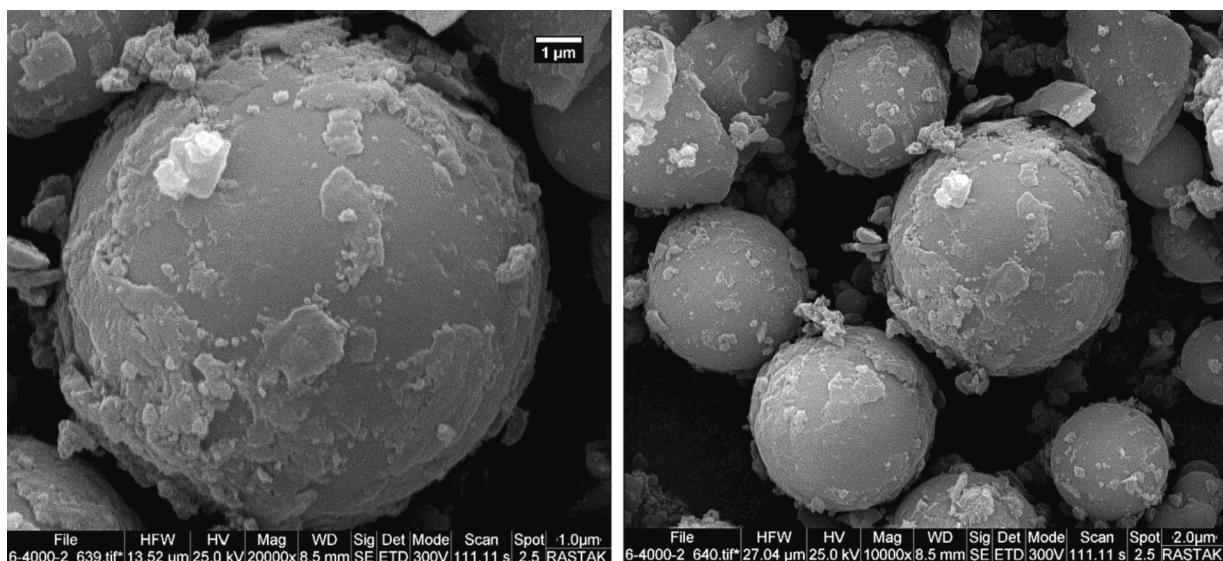
Fig. 12. Scanning electron microscopy (SEM) of reused catalyst.
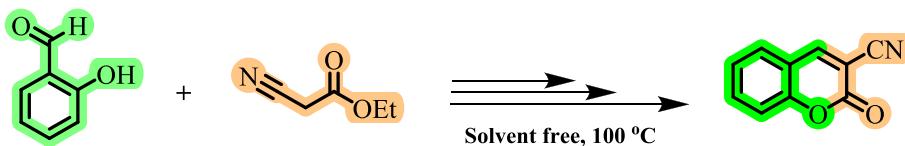
Scheme 5. Preparation of 2-oxo-2*H*-chromene-3-carbonitrile.

Upon completion, hot PEG (10 mL) was added, and the catalyst was separated through centrifugation (2000 rpm) for 10 min. In the next step, 10 mL of H_2O was added to the resulting solution to obtain precipitate. Then the pure product was obtained via trituration of the residue by using ethanol and drying under a vacuum (Scheme 2).

4. Conclusions

In summary, the aim was to develop heterogeneous porous catalysts based on a post-modification strategy. This paper introduces a novel heterogeneous acidic catalyst, Co(BDC-NH(CH$_2$)$_4$SO$_3$H), based on a metal–organic framework utilizing sultone in its synthesis. The structure and morphology of Co(BDC-NH(CH$_2$)$_4$SO$_3$H) were thoroughly investigated and validated through various techniques, including FT-IR, XRD, BET & BJH, SEM, TEM, EDX, Elemental mapping and TGA & DTG. Co (BDC-NH(CH$_2$)$_4$SO$_3$H) demonstrated its catalytic capability in the synthesis of chromeno[4,3-*d*]pyrimidines under mild reaction conditions, with a short reaction period, high efficiency, and without generating by-products. In the structure of the synthesized compounds, two biological moieties such as pyrimidine and chromene were used. Another feature of the synthesized catalyst was its recyclability, which gave it a special feature. Notably, the described reaction marks the first report of a back-to-back anomeric-based oxidation.

Declaration of competing interest

The authors declare that they have no known competing financial interests or personal relationships that could have appeared to influence the work reported in this paper.

Acknowledgments

Appendix A. Supplementary material

Supplementary data to this article can be found online at https://doi.org/10.1016/j.arabjc.2024.105635.

References

Abd El-Mawgoud, H.K., Radwan, H.A.M., El-Mariah, F., et al., 2018. Synthesis, characterization, biological activity of novel 1*H*-benzo [*f*]-chromene and 12*H*-benzo [*f*] chromeno [2, 3-*d*] pyrimidine derivatives. Lett. Drug. Des. Discov. 15, 857–865.

Afsar, J., Zolfigol, M.A., Khazaei, A., et al., 2018. Synthesis and application of a novel nanomagnetic catalyst with Cl[DABCO-NO$_2$]C(NO$_2$)$_3$ tags in the preparation of pyrazolo [3, 4-*b*] pyridines via anomeric based oxidation. Res. Chem. Intermed. 44, 7595–7618.

Afsar, J., Zolfigol, M.A., Khazaei, A., et al., 2020. Synthesis and application of melamine-based nano catalyst with phosphonic acid tags in the synthesis of (3-indolyl) pyrazolo [3, 4-*b*] pyridines via vinylogous anomeric based oxidation. J. Mol. Catal. 482, 110666.

Ahmadi, H., Zarei, M., Zolfigol, M.A., 2022. Catalytic application of a novel basic alkane-sulfonate metal-organic frameworks in the preparation of pyrido [2, 3-*d*] pyrimidines via a cooperative vinylogous anomeric-based oxidation. ChemistrySelect 7, e202202155.

Ahmed, O.M., Mohamed, M.A., Ahmed, R.R., et al., 2009. Synthesis and anti-tumor activities of some new pyridines and pyrazolo [1, 5-*a*] pyrimidines. Eur. J. Med. Chem. 44, 3519–3523.

Alabugin, I.V., Kuhn, L., Medvedev, M.G., et al., 2021. Stereoelectronic power of oxygen in control of chemical reactivity: the anomeric effect is not alone. Chem. Soc. Rev. 50, 10253–10345.

Al-Omar, M.A., Youssef, K.M., El-Sherbeny, M.A., et al., 2005. Synthesis and in vitro antioxidant activity of some new fused pyridine analogs. Archiv der Pharmazie: Eur J. Med. Chem. 338, 175–180.

Aly, H.M., Kamal, M.M., 2012. Efficient one-pot preparation of novel fused chromeno [2, 3-*d*] pyrimidine and pyrano [2, 3-*d*] pyrimidine derivatives. Eur. J. Med. Chem. 47, 18–23.

Arabbaghi, E.K., Mokhtari, J., Naimi-Jamal, M.R., et al., 2021. Zn-MOF: An efficient drug delivery platform for the encapsulation and releasing of Imatinib Mesylate. J. Porous Mater. 28, 641–649.

Atkins, T.J., 1980. Tricyclic trisaminomethanes. J. Am. Chem. Soc. 102, 6364–6365.

Babaee, S., Zolfigol, M.A., Zarei, M., et al., 2018. 1, 10-phenanthroline-based molten salt as a bifunctional sulfonic acid catalyst: application to the synthesis of *N*-heterocycle compounds via anomeric based oxidation. ChemistrySelect 3, 8947–8954.

Babaee, S., Zarei, M., Sepehrmansourie, H., et al., 2020. Synthesis of metal–organic frameworks MIL-101 (Cr)-NH₂ containing phosphorous acid functional groups: application for the synthesis of N-Amino-2-pyridone and pyrano [2, 3-*c*] pyrazole derivatives via a cooperative vinylogous anomeric-based oxidation. ACS Omega 5, 6240–6249.

Babaee, S., Zarei, M., Zolfigol, M.A., et al., 2021. Synthesis of biological based hennotannic acid-based salts over porous bismuth coordination polymer with phosphorous acid tags. RSC Adv. 11, 2141–2157.

Bai, C.-B., Wang, N.-X., Xing, Y., et al., 2017. Progress on chiral NAD (P) H model compounds. Synlett 28, 402–414.

Bassanini, I., Ferrandi, E., Riva, S., et al., 2020. Biocatalysis with laccases: an updated overview. Catalysts 2021 (11), 26.

Bhardwaj, M., Kour, M., Paul, S., 2016. Cu(0) onto sulfonic acid functionalized silica/carbon composites as bifunctional heterogeneous catalysts for the synthesis of polysubstituted pyridines and nitriles under benign reaction media. RSC Adv. 6, 99604–99614.

Biswas, S., Maes, M., Dhakshinamoorthy, A., et al., 2012. Fuel purification, Lewis acid and aerobic oxidation catalysis performed by a microporous Co-BTT (BTT³⁻=1,3, 5-benzenetristetrazolate) framework having coordinatively unsaturated sites. J. Mater. Chem. 22, 10200–10209.

Boselli, L., Ader, I., Carraz, M., et al., 2014. Synthesis, structures, and selective toxicity to cancer cells of gold (I) complexes involving N-heterocyclic carbene ligands. Eur. J. Med. Chem. 85, 87–94.

Buazar, F., Sayahi, M.H., Zarei Sefiddashti, A., 2023. Marine carrageenan-based NiO nanocatalyst in solvent-free synthesis of polyhydroquinoline derivatives. Appl. Organomet. Chem. 37, e7191.

Bueno, J.M., Carda, M., Crespo, B., et al., 2016. Design, synthesis and antimalarial evaluation of novel thiazole derivatives. Bioorganic Med. Chem. Lett. 26, 3938–3944.

Catlin, D.H., Sekera, M.H., Ahrens, B.D., et al., 2004. Tetrahydrogestrinone: discovery, synthesis, and detection in urine. Rapid Commun. Mass Spectrom. 18, 1245-1049.

Dhakshinamoorthy, A., Asiri, A.M., Garcia, H., 2020b. Metal–organic frameworks as multifunctional solid catalysts. Trends Chem. 2, 454–466.

Dhakshinamoorthy, A., Garcia, H., 2014. Metal–organic frameworks as solid catalysts for the synthesis of nitrogen-containing heterocycles. Chem. Soc. Rev. 43, 5750–5765.

Dhakshinamoorthy, A., Asiri, A.M., Garcia, H., 2020a. Catalysis in confined spaces of metal organic frameworks. ChemCatChem 12, 4732–4753.

Dondoni, A., Marra, A., 2000. Methods for anomeric carbon-linked and fused sugar amino acid synthesis: the gateway to artificial glycopeptides. Chem. Rev. 100, 4395–4422.

Erhardt, J.M., Grover, E.R., Wuest, J.D., 1980. Transfer of hydrogen from orthoamides. Synthesis, structure, and reactions of hexahydro-6bH-2a, 4a, 6a-triazacyclopenta [cd] pentalene and perhydro-3a, 6a, 9a-triazaphenalene. J. Am. Chem. Soc. 102, 6365–6369.

Erhardt, J.M., Wuest, J.D., 1980. Transfer of hydrogen from orthoamides. Reduction of protons to molecular hydrogen. J. Am. Chem. Soc. 102, 6363–6364.

Furdui, B., Parfene, G., Ghinea, I.O., et al., 2014. Synthesis and in vitro antimicrobial evaluation of new *N*-heterocyclic diquaternary pyridinium compounds. Molecules 19, 11572–11585.

Furukawa, H., Cordova, K.E., O'Keeffe, M., et al., 2013. The chemistry and applications of metal-organic frameworks. Science 341, 1230444.

Gao, F., Yan, R., Shu, Y., et al., 2022. Strategies for the application of metal–organic frameworks in catalytic reactions. RSC Adv. 12, 10114–10125.

Hamasaka, G., Tsuji, H., Uozumi, Y., 2015. Organoborane-catalyzed hydrogenation of unactivated aldehydes with a Hantzsch ester as a synthetic NAD (P)H analogue. Synlett 26, 2037–2041.

He, T., Shi, R., Gong, Y., et al., 2016. Base-promoted cascade approach for the preparation of reduced knoevenagel adducts using hantzsch esters as reducing agent in water. Synlett 27, 1864–1869.

Hese, S.V., Meshram, R.J., Kamble, R.D., et al., 2017. Antidiabetic and allied biochemical roles of new chromeno-pyrano pyrimidine compounds: synthesis, in vitro and in silico analysis. Med. Chem. Res. 26, 805–818.

Jalili, F., Zarei, M., Zolfigol, M.A., et al., 2020. SBA-15/PrN(CH₂PO₃H₂)₂ as a novel and efficient mesoporous solid acid catalyst with phosphorous acid tags and its application on the synthesis of new pyrimido [4, 5-*b*] quinolines and pyrido [2, 3-*d*] pyrimidines via anomeric based oxidation. Microporous Mesoporous Mater. 294, 109865.

Jalili, F., Zarei, M., Zolfigol, M.A., et al., 2022. Application of novel metal–organic framework [Zr-UiO-66-PDC-SO₃H]FeCl₄ in the synthesis of dihydrobenzo [g] pyrimido [4, 5-b] quinoline derivatives. RSC Adv. 12, 9058–9068.

Kalhor, S., Yarie, M., Rezaeivala, M., et al., 2019. Novel magnetic nanoparticles with morpholine tags as multirole catalyst for synthesis of hexahydroquinolines and 2-amino-4, 6-diphenylnicotinonitriles through vinylogous anomeric-based oxidation. Res. Chem. Intermed. 45, 3453–3480.

Kalhor, S., Zarei, M., Sepehrmansourie, H., et al., 2021a. Novel uric acid-based nano organocatalyst with phosphorous acid tags: application for synthesis of new biologically-interest pyridines with indole moieties via a cooperative vinylogous anomeric based oxidation. J. Mol. Catal. 507, 111549.

Kalhor, S., Zarei, M., Zolfigol, M.A., et al., 2021b. Anodic electrosynthesis of MIL-53(Al)-N(CH₂PO₃H₂)₂ as a mesoporous catalyst for synthesis of novel (*N*-methyl-pyrrol)-pyrazolo [3, 4-b] pyridines via a cooperative vinylogous anomeric based oxidation. Sci. Rep. 11, 19370.

Kamdar, N.R., Haveliwala, D.D., Mistry, P.T., et al., 2011. Synthesis and evaluation of in vitro antitubercular activity and antimicrobial activity of some novel 4*H*-chromeno [2, 3-*d*] pyrimidine via 2-amino-4-phenyl-4*H*-chromene-3-carbonitriles. Med. Chem. Res. 20, 854–864.

Kiafar, M., Zolfigol, M.A., Yarie, M., et al., 2016. The first computational study for the oxidative aromatization of pyrazolines and 1, 4-dihydropyridines using 1, 2, 4-triazolinediones: an anomeric-based oxidation. RSC Adv. 6, 102280–102291.

Kumar, R.S., Idhayadhulla, A., Nasser, A.J.A., et al., 2010. Synthesis and anticonvulsant activity of a new series of 1, 4-dihydropyridine derivatives. Indian J. Pharm. Sci. 72, 719.

Lang, R.W., Wenk, P.F., 1988. Synthesis of selectively trifluoromethylated pyridine derivaties as potential antihypertensives. Helv. Chim. Acta 71, 596–601.

MacGillivray, L.R., 2010. Metal-organic frameworks: design and application. John Wiley & Sons.

Masoomi, M.Y., Bagheri, M., Morsali, A., 2015. Application of two cobalt-based metal–organic frameworks as oxidative desulfurization catalysts. Inorg. Chem. 54, 11269–11275.

Metobo, S.E., Jin, H., Tsiang, M., et al., 2006. Design, synthesis, and biological evaluation of novel tricyclic HIV-1 integrase inhibitors by modification of its pyridine ring. Bioorganic Med. Chem. Lett. 16, 3985–3988.

Miljkovic, M., 2009. Carbohydrates: synthesis, mechanisms, and stereoelectronic effects. Springer Science & Business Media.

Miljkovic, M., Miljković, M., 2009. Anomeric Effect. Synthesis, Mechanisms, and Stereoelectronic Effects, Carbohydrates, pp. 57–93.

Moavi, J., Buazar, F., Sayahi, M.H., 2021. Algal magnetic nickel oxide nanocatalyst in accelerated synthesis of pyridopyrimidine derivatives. Sci. Rep. 11, 6296.

Moosavi-Zare, A.R., Zolfigol, M.A., Zarei, M., et al., 2013. Design, characterization and application of new ionic liquid 1-sulfopyridinium chloride as an efficient catalyst for tandem Knoevenagel-Michael reaction of 3-methyl-1-phenyl-1*H*-pyrazol-5 (4*H*)-one with aldehydes. Appl. Catal. A 467, 61–68.

Moosavi-Zare, A.R., Zolfigol, M.A., Rezanejad, Z., 2016. Trityl chloride promoted the synthesis of 3-(2, 6-diarylpyridin-4-yl)-1H-indoles and 2, 4, 6-triarylpyridines by in situ generation of trityl carbocation and anomeric based oxidation in neutral media. Can. J. Chem. 94, 626–630.

Naseri, A.M., Zarei, M., Alizadeh, S., et al., 2021. Synthesis and application of [Zr-UiO-66-PDC-SO₃H]Cl MOFs to the preparation of dicyanomethylene pyridines via chemical and electrochemical methods. Sci. Rep. 11, 16817.

Rajanarendar, E., Reddy, M.N., Krishna, S.R., et al., 2012. Design, synthesis, antimicrobial, anti-inflammatory and analgesic activity of novel isoxazolyl pyrimido [4, 5-*b*] quinolines and isoxazolyl chromeno [2, 3-*d*] pyrimidin-4-ones. Eur. J. Med. Chem. 55, 273–283.

Safaei, M., Foroughi, M.M., Ebrahimpoor, N., et al., 2019. A review on metal-organic frameworks: Synthesis and applications. TrAC. Trends Anal. Chem. 118, 401–425.

Saghanezhad, S.J., Sayahi, M.H., Imanifar, I., et al., 2017. Caffeine-H₃PO₄: a novel acidic catalyst for various one-pot multicomponent reactions. Res. Chem. Intermed. 43, 6521–6536.

Saikia, M., Saikia, L., 2016. Sulfonic acid-functionalized MIL-101(Cr) as a highly efficient heterogeneous catalyst for one-pot synthesis of 2-amino-4 H-chromenes in aqueous medium. RSC Adv. 6, 15846–15853.

Sayahi, M.H., Bahadorikhalili, S., Saghanezhad, S.J., et al., 2018a. Copper(II)-supported polyethylenimine-functionalized magnetic graphene oxide as a catalyst for the green synthesis of 2-arylquinazolin-4 (3*H*)-ones. Res. Chem. Intermed. 44, 5241–5253.

Sayahi, M.H., Saghanezhad, S.J., Mahdavi, M., 2018b. SBA-15-SO₃H-assisted preparation of 4-aza-phenanthrene-3, 10-dione derivatives via a one-pot, four-component reaction. Res. Chem. Intermed. 44, 739–747.

Sayahi, M.H., Saghanezhad, S.J., Bahadorikhalili, S., et al., 2019a. CuBr-catalysed one-pot multicomponent synthesis of 3-substituted 2-thioxo-2, 3-dihydroquinazolin-4 (1*H*)-one derivatives. Appl. Organomet. Chem. 33, e4635.

Sayahi, M.H., Saghanezhad, S.J., Mahdavi, M., 2019b. Catalyst-free three-component synthesis of 2-amino-4, 6-diarylpyridine-3-carbonitriles under solvent-free conditions. Chem. Heterocycl. 55, 725–728.

Sayahi, M.H., Bahadorikhalili, S., Saghanezhad, S.J., et al., 2020. Sulfonic acid-functionalized poly (4-styrenesulfonic acid) mesoporous graphene oxide hybrid for one-pot preparation of coumarin-based pyrido [2, 3-*d*] pyrimidine-dione derivatives. Res. Chem. Intermed. 46, 491–507.

Sayahi, M.H., Ghomi, M., Hamad, S.M., et al., 2021a. Electrochemical synthesis of three-dimensional flower-like Ni/Co–BTC bimetallic organic framework as heterogeneous catalyst for solvent-free and green synthesis of substituted chromeno [4, 3–*b*] quinolones. J. Chin. Chem. Soc. 68, 620–629.

Sayahi, M.H., Shamkhani, F., Mahdavi, M., et al., 2021b. Efficient synthesis of chromeno [4, 3-b] pyrano [3, 4-*e*] pyridine-6, 8-dione derivatives via multicomponent one-pot reaction under mild reaction conditions in water. Res. Chem. Intermed. 47, 4101–4112.

Sayahi, M.H., Shamkhani, F., Mahdavi, M., et al., 2021c. Sulfonic acid functionalized magnetic starch as an efficient catalyst for the synthesis of chromeno [4, 3-b] quinoline-6, 8 (9*H*)-dione derivatives. Starch-Stärke. 73, 2000257.

Sayahi, M.H., Afrouzandeh, Z., Bahadorikhalili, S., 2022a. Cu(OAc)₂ catalyzed synthesis of novel chromeno [4, 3-b] pyrano [3, 4-*e*] pyridine-6, 8-dione derivatives via a one-pot multicomponent reaction in water under mild reaction conditions. Polycycl. Aromat. Compd. 42, 3391–3400.

Sayahi, M.H., Toosibashi, M., Bahmaei, M., et al., 2022b. Pd@ Py₂PZ@MSN as a novel and efficient catalyst for C-C bond formation reactions. Front. Chem. 10, 838294.

Sayahi, M.H., Sepahdar, A., Bazrafkan, F., et al., 2023. Ionic liquid modified SPION@ chitosan as a novel and reusable superparamagnetic catalyst for green one-pot synthesis of pyrido [2, 3-d] pyrimidine-dione derivatives in water. Catalysts 13, 290.

Sepehrmansouri, H., Zarei, M., Zolfigol, M.A., et al., 2020. Multilinker phosphorous acid anchored En/MIL-100 (Cr) as a novel nanoporous catalyst for the synthesis of new *N*-heterocyclic pyrimido [4, 5-*b*] quinolines. J. Mol. Catal. 481, 110303.

Sepehrmansourie, H., 2020. Spotlight: silica sulfuric acid (SSA): as a multipurpose catalyst. Iran. J. Catal. 10, 175–179.

Sepehrmansourie, H., 2021. Spotlight: metal organic frameworks (MOFs): as multi-purpose catalysts. Iran. J. Catal. 11, 207–215.

Sepehrmansourie, H., Zarei, M., Zolfigol, M.A., et al., 2021. Application of novel nanomagnetic metal–organic frameworks as a catalyst for the synthesis of new pyridines and 1, 4-dihydropyridines via a cooperative vinylogous anomeric based oxidation. Sci. Rep. 11, 5279.

Sepehrmansourie, H., Zarei, M., Zolfigol, M.A., et al., 2022. Catalytic chemo and homoselective ipso-nitration under mild condition. J. Mol. Catal. 531, 112634.

Sepehrmansourie, H., Alamgholiloo, H., Pesyan, N.N., et al., 2023. A MOF-on-MOF strategy to construct double Z-scheme heterojunction for high-performance photocatalytic degradation. Appl Catal B 321, 122082.

Tabacchi, G., Vanoni, M.A., Gamba, A., et al., 2007. Does negative hyperconjugation assist enzymatic dehydrogenations? ChemPhysChem 8, 1283–1288.

Tavakoli, E., Sepehrmansourie, H., Zarei, M., et al., 2022. Applications of novel composite UiO-66-NH$_2$/Melamine with phosphorous acid tags as a porous and efficient catalyst for the preparation of novel spiro-oxindoles. New J. Chem. 46, 19054–19061.

Vannice, M.A., Joyce, W.H., 2005. Kinetics of catalytic reactions. Springer.

Xu, C., Fang, R., Luque, R., et al., 2019. Functional metal–organic frameworks for catalytic applications. Coord. Chem. Rev. 388, 268–292.

Yang, D., Gates, B.C., 2019. Catalysis by metal organic frameworks: perspective and suggestions for future research. ACS Catal. 9, 1779–1798.

Yang, Y., Lin, R., Ge, L., et al., 2015. Synthesis and characterization of three amino-functionalized metal–organic frameworks based on the 2-aminoterephthalic ligand. Dalton Trans. 44, 8190–8197.

Yarie, M., 2017. Catalytic anomeric based oxidation. Iran. J. Catal. 7, 85–88.

Yarie, M., 2020. Spotlight: Catalytic vinylogous anomeric based oxidation (Part I). Iran. J. Catal. 10, 79–83.

Yavuz, S.Ç., Akkoç, S., Tüzün, B., et al., 2021. Efficient synthesis and molecular docking studies of new pyrimidine-chromeno hybrid derivatives as potential antiproliferative agents. Synth. Commun. 51, 2135–2159.

Yu, G., Sun, J., Muhammad, F., et al., 2014. Cobalt-based metal organic framework as precursor to achieve superior catalytic activity for aerobic epoxidation of styrene. RSC Adv. 4, 38804–38811.

Zefirov, N.S., Shekhtman, N.M., 1971. The anomeric effect. Russ. Chem. Rev. 40, 315.

Zhang, X., Han, J., Guo, J., et al., 2021b. Engineering nanoscale metal-organic frameworks for heterogeneous catalysis. Small Structures. 2, 2000141.

Zhang, L.-J., Yang, M.-Y., Sun, Z.-H., et al., 2014. Synthesis and antifungal activity of 1, 3, 4-thiadiazole derivatives containing pyridine group. Lett. Drug. Des. Discov. 11, 1107–1111.

Zhang, H., Yang, L.-M., Ganz, E., 2020. Adsorption properties and microscopic mechanism of CO$_2$ capture in 1, 1-dimethyl-1, 2-ethylenediamine-grafted metal-organic frameworks. ACS Appl. Mater. Interfaces 12, 18533–18540.

Zhang, H., Zheng, X., Yang, L.-M., et al., 2021a. Properties and detailed adsorption of CO$_2$ by M$_2$ (dobpdc) with N, N-dimethylethylenediamine functionalization. Inorg. Chem. 60, 2656–2662.

Zhao, X., Xiao, J., Tang, W., 2017. Enantioselective reduction of 3-substituted quinolines with a cyclopentadiene-based chiral Brønsted acid. Synthesis 49, 3157–3164.

Zippel, C., Seibert, J., Bräse, S., 2021. Skeletal editing—nitrogen deletion of secondary amines by anomeric amide reagents. Angew. Chem Int. Ed. Engl. 60, 19522–19524.

Zolfigol, M.A., 2001. Silica sulfuric acid/NaNO$_2$ as a novel heterogeneous system for production of thionitrites and disulfides under mild conditions. Tetrahedron 57, 9509–9511.

Zolfigol, M.A., Karimi, F., Yarie, M., et al., 2018b. Catalytic application of sulfonic acid-functionalized titana-coated magnetic nanoparticles for the preparation of 1, 8-dioxodecahydroacridines and 2, 4, 6-triarylpyridines via anomeric-based oxidation. Appl. Organomet. Chem. 32, e4063.

Zolfigol, M., Khazaei, A., Karimitabar, F., et al., 2018a. Synthesis of Indolo [3, 2-*b*] carbazoles via an anomeric-based oxidation process: a combined experimental and computational strategy. J. Heterocycl. Chem. 55, 1061–1068.

Zolfigol, M.A., Safaiee, M., Afsharnadery, F., et al., 2015. Silica vanadic acid [SiO$_2$–VO(OH)$_2$] as an efficient heterogeneous catalyst for the synthesis of 1, 2-dihydro-1-aryl-3 *H*-naphth [1, 2-*e*][1, 3] oxazin-3-one and 2, 4, 6-triarylpyridine derivatives via anomeric based oxidation. RSC Adv. 5, 100546–100559.

Zolfigol, M.A., Yarie, M., 2017. Fe$_3$O$_4$@TiO$_2$@O$_2$PO$_2$(CH$_2$)NHSO$_3$H as a novel nanomagnetic catalyst: Application to the preparation of 2-amino-4, 6-diphenylnicotinonitriles via anomeric-based oxidation. Appl. Organomet. Chem. 31, e3598.